RESEARCH PAPER

To Develop And Evaluate A Targeted Nanosuspension of Curcumin And Silimarin To Enhance Their Bioavailability, Cellular Uptake, And Anticancer Efficacy Against Cervical Cancer

Shaikh Alphiya Abbas[1*], Bhati Varsha Rajendra[2], Jadhav Pooja[3], Kote Sonali Rajendra[4], Kawade Dadasaheb M.[5], Kulkarni Prasanna Santosh[6], Kale Pratik Ravindra[7]

[1,2]Department of Pharmaceutics, Rashtrasant Janardhan Swami College of Pharmacy, Kokamthan, Tal- Kopargaon, Dist. Ahilyanagar, Maharashtra, 423601, India

[3,4,5]Department of Pharmaceutical Chemistry, Rashtrasant Janardhan Swami College of Pharmacy, Kokamthan, Tal- Kopargaon, Dist. Ahilyanagar, Maharashtra, 423601, India

[6,7]Rashtrasant Janardhan Swami College of Pharmacy, Kokamthan, Tal- Kopargaon, Dist. Ahilyanagar, Maharashtra, 423601, India

Address for Correspondence:

Shaikh Alphiya Abbas*

Address: Department of Pharmaceutics, Rashtrasant Janardhan Swami College of Pharmacy, Kokamthan, Tal- Kopargaon, Dist. Ahilyanagar, Maharashtra, 423601, India

E-mail-Id: alphiyaashaikh@gmail.com

Received: 14th May, 2026; Revised: 27th May 2026; Accepted: 23th Jun, 2026; Available Online: 12th July, 2026

ABSTRACT:

Cervical cancer remains one of the leading causes of cancer-related mortality among women worldwide, particularly in developing countries. Although conventional treatments such as chemotherapy, radiotherapy, and surgery are available, their effectiveness is often limited by systemic toxicity, multidrug resistance, and poor targeting of cancer cells. Natural phytoconstituents such as Curcumin and Silymarin have demonstrated significant anticancer, antioxidant, and anti-inflammatory activities against various malignancies, including cervical cancer. Curcumin inhibits multiple signaling pathways involved in tumor growth, angiogenesis, and metastasis, while Silymarin suppresses oxidative stress and promotes apoptosis in cancer cells. However, their therapeutic application is restricted due to poor aqueous solubility, low permeability, rapid metabolism, and limited bioavailability.

The present study focuses on the development of a targeted Curcumin–Silymarin nanosuspension to enhance solubility, cellular uptake, and therapeutic efficacy against cervical cancer. The nanosuspension is prepared using nanoprecipitation or high-speed homogenization techniques with stabilizers such as polyvinyl pyrrolidone (PVP), poloxamer, and Tween 80 to ensure particle stability and prevent aggregation. The formulation is optimized by varying process parameters and evaluated for particle size, polydispersity index, zeta potential, morphology, entrapment efficiency, drug content, saturation solubility, and in vitro drug release. Anticancer activity is assessed using HeLa cervical cancer cell lines through cytotoxicity, apoptosis, cellular uptake, and cell viability studies. The nanosized formulation is expected to improve drug dissolution, enhance intracellular delivery, and provide synergistic anticancer effects. These findings suggest that Curcumin–Silymarin nanosuspension may serve as a promising targeted nanocarrier system for effective cervical cancer therapy.

KEYWORDS: Cervical Cancer, Curcumin–Silymarin Nanosuspension, Targeted Drug Delivery, Anticancer Activity

How to cite this article: Abbas SA, Bhati VR, Jadhav P, Kote SR, Kawade DM, Kulkarni PS, Kale PR. To Develop And Evaluate A Targeted Nanosuspension of Curcumin And Silymarin To Enhance Their Bioavailability, Cellular Uptake, And Anticancer Efficacy Against Cervical Cancer. Int J Drug Deliv Technol. 2026;16(69s):1190-1205. DOI: 10.25258/ijddt.16.69s.120

INTRODUCTION:

Cervical cancer is one of the most common cancers affecting women worldwide And remains a major public health concern, especially in developing countries.Cervical cancer is a malignant disease that develops in the cells of the cervix, the lower part of the uterus that connects to the vagina. It is one of the most common cancers affecting women . The primary cause of cervical cancer is persistent infection with high-risk types of the human papillomavirus (HPV), which is transmitted mainly through sexual contact.

The primary cause of cervical cancer is persistent infection with Human Papillomavirus (HPV), a common sexually transmitted virus. Among the many HPV types, high-risk strains—especially HPV-16 and HPV-18—are responsible for about 70% of cervical cancer cases. The virus can cause changes in cervical cells by interfering with normal cell

HPV-positive cell lines

HeLa → HPV-18 positive

SiHa → HPV-16 positive (low viral copy number)

CaSki → HPV-16 positive (high viral copy number) cycle control, leading to uncontrolled cell growth and, eventually, cancer. Vaccination against HPV and regular screening are effective strategies for preventing cervical cancer.

Curcumin

A bioactive compound obtained from Curcuma longa (turmeric), is well known for its anti-inflammatory, antioxidant, antiviral, and anticancer properties. Research has shown that curcumin can inhibit the expression of HPV oncogenes E6 and E7, restore tumor suppressor proteins, and induce apoptosis in infected cells. Due to these properties, curcumin is being investigated as a potential natural agent for the management of HPV-associated infections and cancers.

Monograph of Curcumin

Name : Curcumin

Biological Source

Curcumin is obtained from the dried rhizomes of Curcuma longa Linn.
Family: Zingiberaceae

Geographical Source

India (major producer), China, Indonesia, Sri Lanka, Thailand

Chemical Nature

Curcumin is a polyphenolic diarylheptanoid and the principal curcuminoid of turmeric.
Chemical formula: $C_{21}H_{20}O_6$
Molecular weight: 368.38 g/mol

Chemical Structure

Curcumin consists of two aromatic rings with o-methoxy phenolic groups connected by a seven-carbon linker containing α,β-unsaturated diketone moiety.

Physical Properties

Appearance: Yellow to orange crystalline powder
Odor: Slight
Taste: Bitter

Solubility: Insoluble in water; soluble in ethanol, acetone, chloroform
Melting point: ~183°C

Identification Tests

Produces reddish-brown color with alkali
Gives yellow coloration in acidic medium
UV absorption maximum at ~425 nm

Chemical Constituents

Curcumin (major)
Demethoxycurcumin
Bisdemethoxycurcumin
Volatile oils (turmerone, atlantone, zingiberene)

Pharmacological Actions

Anti-inflammatory
Antioxidant
Antimicrobial
Anticancer (chemopreventive)
Hepatoprotective
Neuroprotective

Mechanism of Action

Curcumin modulates multiple signaling pathways including NF-κB, COX-2, TNF-α, and various cytokines, leading to reduced inflammation and oxidative stress.

Therapeutic Uses

Inflammatory disorders (arthritis)
Digestive disorders
Liver diseases
Wound healing
Adjunct in cancer therapy
Skin diseases
Bioavailability
Curcumin has poor oral bioavailability due to low absorption and rapid metabolism. Bioavailability is enhanced when combined with piperine.

Dose

Oral: 500–2000 mg/day (in divided doses, standardized extract)
Topical: As required

Adverse Effects

Generally safe; high doses may cause:
Gastrointestinal upset
Nausea
Diarrhea

Contraindications

Gallstones or bile duct obstruction
Pregnancy (high doses)

Storage

Store in a cool, dry place, protected from light and moisture.

SILIMARIN

Silymarin is a natural flavonoid complex extracted from the seeds of the medicinal plant Silybum marianum, commonly known as milk thistle. It is composed mainly of active constituents such as silybin (silibinin), isosilybin, silychristin, and

silydianin. Among these, silibinin is considered the most biologically active component.
Traditionally, silymarin has been widely used for its hepatoprotective (liver-protecting), antioxidant, and anti-inflammatory properties. In recent years, it has gained attention in the field of cancer research due to its potential anticancer effects

Monograph of silimarin

1. Name of Drug
Generic Name: Silymarin

Synonyms: Milk Thistle Extract

Biological Source: Obtained from seeds of Silybum marianum

2. Family
Asteraceae (Compositae)

3. Chemical Constituents
Silymarin is a mixture of flavonolignans:

Silybin (Silibinin) – major active component

Isosilybin ,Silychristin ,Silydianin

Molecular Formula (Silybin): $C_{25}H_{22}O_{10}$
Molecular Weight: ~482.44 g/mol

4. Description
Yellow to brown crystalline powder
Odorless or faint odor
Slightly bitter taste

5. Solubility

Poorly soluble in water
Soluble in ethanol, methanol, and acetone

6. Identification Tests
Chemical test: Gives positive fl…

OBJECTIVE:

1. To develop a nanosuspension formulation of curcumin and silymarin using suitable stabilizers and preparation techniques.
2. To enhance the aqueous solubility and dissolution rate of curcumin and silymarin through nanosuspension technology.
3. To improve the oral bioavailability of curcumin and silymarin by reducing particle size to the nanometer range.
4. To incorporate a targeting mechanism (e.g., ligand-based or passive targeting) for improved delivery to cervical cancer cells.
5. To evaluate the physicochemical properties of the nanosuspension, including particle size, zeta potential, polydispersity index (PDI), and morphology.
6. To assess the stability of the developed nanosuspension under different storage conditions.
7. To study the in vitro drug release profile of curcumin and silymarin from the nanosuspension.
8. To evaluate cellular uptake of the nanosuspension in cervical cancer cell lines.

MATERIALS AND METHODS:

Materials

Curcumin (CUR, purity ≥ 98%) and Silymarin (SIL, standardized to ≥ 70% Silybin) were procured from Sigma-Aldrich (St. Louis, MO, USA). PVP (Lutrol F-127), D-alpha-tocopheryl polyethylene glycol 1000 succinate (TPGS), Polyvinyl Alcohol (PVA, MW 31,000–50,000), and Polyvinylpyrrolidone K-30 (PVP K-30) were obtained from BASF SE (Ludwigshafen, Germany). Soy Lecithin (Phospholipon 90G) was supplied by Lipoid GmbH (Ludwigshafen, Germany). Propylene glycol (PG) and Dimethyl Sulfoxide (DMSO) were procured from Merck KGaA (Darmstadt, Germany). Acetonitrile (HPLC grade), Methanol (HPLC grade), and all other analytical-grade solvents were purchased from Fisher Scientific (Pittsburgh, PA, USA). HeLa human cervical carcinoma cell line was obtained from the National Centre for Cell Science (NCCS), Pune, India. Dulbecco's Modified Eagle Medium (DMEM), Fetal Bovine Serum (FBS), penicillin-streptomycin solution, trypsin-EDTA, and Phosphate Buffered Saline (PBS, pH 7.4) were procured from HiMedia Laboratories (Mumbai, India). 3-(4,5-Dimethylthiazol-2-yl)-2,5-diphenyltetrazolium bromide (MTT) reagent was sourced from Sigma-Aldrich. Purified water (18.2 MΩ·cm) was prepared in-house using a Milli-Q system (Millipore, USA). All chemicals and reagents were of pharmacopoeial or analytical grade unless otherwise specified.

Table 1: List of Materials Used in the Study

Material	Grade/Specification	Supplier	Role in Formulation
Curcumin	≥98% purity (HPLC)	Sigma-Aldrich	Active Drug (API)
Silymarin	≥70% Silybin, std.	Sigma-Aldrich	Active Drug (API)
PVP	Pharmaceutical grade	BASF SE	Stabilizer / Surfactant
TPGS (Vit. E PEG 1000)	Pharmaceutical grade	BASF SE	Co-surfactant / P-gp Inhibitor
PVP K-30	Pharmaceutical grade	BASF SE	Cryoprotectant / Stabilizer
PVA (MW 31–50 kDa)	Pharmaceutical grade	Sigma-Aldrich	Steric Stabilizer
Soy Lecithin (P90G)	Pharmaceutical grade	Lipoid GmbH	Emulsifier / Wetting Agent
Propylene Glycol	Pharmaceutical grade	Merck KGaA	Co-solvent
HeLa Cell Line	Human cervical carcinoma	NCCS, Pune	In vitro anticancer study
MTT Reagent	Analytical grade	Sigma-Aldrich	Cell viability assay
DMEM (High Glucose)	Cell culture grade	HiMedia	Cell culture medium

Preparation of CUR-SIL Nanosuspension

Five formulations of Curcumin-Silymarin nanosuspension (F1–F5) were prepared using a solvent-antisolvent precipitation technique coupled with high-pressure homogenization, as described by Bhakay et al. (2018) with modifications. This two-step approach was selected to achieve nanometric particle dimensions with narrow size distribution and optimal colloidal stability without application of thermal stress, which is critical for preserving the bioactivity of thermolabile polyphenolic compounds. The formulations were systematically varied with respect to the drug molar ratio (CUR:SIL), stabilizer concentrations (PVP, TPGS, and Soy Lecithin), and high-pressure homogenization process parameters (pressure and number of cycles), as detailed in Table 4.2. The formulation that yielded the optimal physicochemical attributes smallest particle size, lowest PDI, highest zeta potential magnitude, and maximum entrapment efficiency was designated the optimized formulation (F5).

Step I: Solvent-Antisolvent Precipitation

For each formulation, accurately weighed quantities of Curcumin (50 mg) and Silymarin (50 mg) at the specified molar ratio (Table 4.2) were co-dissolved in 5 mL of DMSO:Methanol (1:1 v/v) (organic phase) under sonication for 15 minutes at 25°C using a probe sonicator (Hielscher UP200St, 200 W, Germany). The organic phase was then injected dropwise (0.5 mL/min) through a syringe pump into 50 mL of the aqueous stabilizer phase containing the respective concentrations of PVP, TPGS, and Soy Lecithin (as per Table 4.2) pre-dissolved in purified water under continuous magnetic stirring at 1000 rpm at 25°C. Instantaneous nanoprecipitation occurred upon contact of the organic and aqueous phases, generating a crude nanosuspension (pre-nanosuspension). Organic solvents were subsequently removed by rotary evaporation (Buchi R-300, Switzerland) at 40°C under reduced pressure (200 mbar) for 30 minutes, followed by nitrogen gas purging for 15 minutes to ensure complete solvent removal.

Step II: High-Pressure Homogenization (HPH)

The pre-nanosuspension was subjected to high-pressure homogenization (Microfluidizer M-110P, Microfluidics Corp., USA) at the specified pressure and number of cycles (Table 4.2) at 4°C (ice-cooled reservoir) to further reduce and homogenize particle size and polydispersity. The resulting nanosuspension was collected and characterized immediately or stored at 4°C in amber glass vials under a nitrogen blanket prior to lyophilization.

Lyophilization (Freeze-Drying)

To enhance long-term stability, all five nanosuspension formulations were lyophilized (Labconco FreeZone 6 Plus, USA). PVP K-30 (5% w/v) was added as a cryoprotectant prior to lyophilization to prevent particle aggregation during the freezing and drying process, as previously demonstrated by Abdelwahed et al. (2006). The suspension was pre-frozen at −80°C for

12 hours; primary drying was performed at −40°C under 0.133 mbar for 24 hours, followed by secondary drying at 25°C under 0.013 mbar for 6 hours. The resultant lyophilized cakes (F1–F5 lyophilizates) were stored in a desiccator at 25°C until use.

Table 2: Composition of Five CUR-SIL Nanosuspension Formulations (F1–F5)

Ingredient	F1	F2	F3	F4	F5 (Optimized)	Role
Curcumin (mg)	50	50	50	50	50	Active API
Silymarin (mg)	50	50	50	50	50	Active API
Drug ratio CUR:SIL	1:1	2:1	1:2	1:1	1:1	Molar ratio
PVP (% w/v)	0.25	0.25	0.25	0.75	0.50	Steric Stabilizer
TPGS (% w/v)	0.05	0.05	0.05	0.20	0.10	Co-surfactant
Soy Lecithin P90G (% w/v)	0.10	0.10	0.10	0.30	0.20	Emulsifier
PVP K-30 (% w/v)	5.0	5.0	5.0	5.0	5.0	Cryoprotectant
HPH Cycles	5	10	10	15	10	Process parameter
HPH Pressure (psi)	15,000	20,000	20,000	20,000	20,000	Process parameter

F5 = Optimized formulation selected on the basis of physicochemical characterization results. HPH = High-Pressure Homogenization; TPGS = D-α-tocopheryl polyethylene glycol 1000 succinate.

Characterization Methods

All five nanosuspension formulations (F1–F5) were subjected to comprehensive physicochemical characterization as described below. Each characterization method was applied uniformly to all formulations to enable systematic comparison and selection of the optimal formulation (F5).

1.Particle Size and Polydispersity Index (PDI) by Dynamic Light Scattering (DLS)

Mean particle size (Z-average diameter) and polydispersity index (PDI) of each nanosuspension formulation were determined by Dynamic Light Scattering (DLS) using a Malvern Zetasizer Nano ZS instrument (Malvern Instruments Ltd., Worcestershire, UK) equipped with a 4 mW He-Ne laser (λ = 633 nm) at a fixed backscattering angle of 173°. Prior to measurement, each nanosuspension was diluted 1:100 with purified water (previously filtered through a 0.22 µm PVDF membrane filter) to achieve a suitable scattering count rate (200–500 kcps). All measurements were conducted at 25°C following 2 minutes of equilibration, and results represent the mean ± standard deviation (SD) of three independent measurements (n = 3). PDI values < 0.2 were considered indicative of a narrow, monodisperse size distribution suitable for pharmaceutical nanosystems.

2. Zeta Potential

Zeta potential (ζ) of each CUR-SIL nanosuspension formulation was determined by Electrophoretic Light Scattering (ELS) using the same Malvern Zetasizer Nano ZS instrument equipped with a folded capillary zeta cell (DTS1070). Each nanosuspension formulation was diluted 1:200 in 10 mM NaCl solution (adjusted to physiological ionic strength) before analysis. Measurements were performed in automatic mode using the Smoluchowski approximation at 25°C. A minimum of 3 measurements per sample were performed, and data are expressed as mean ± SD. Zeta potential values ≤ −25 mV or ≥ +25 mV were considered indicative of adequate electrostatic repulsion and colloidal stability, in accordance with DLVO theory.

3. Drug Content Determination

Drug content of each lyophilized nanosuspension formulation was determined spectrophotometrically. An accurately weighed aliquot of each lyophilized nanosuspension equivalent to 10 mg total drug (CUR + SIL) was dissolved in 10 mL DMSO and subjected to probe sonication for 10 minutes to ensure complete dissolution. The resulting solution was diluted appropriately with methanol:water (70:30 v/v, pH 6.8). Curcumin content was determined at 425 nm and Silymarin content at 288 nm using a UV–Vis spectrophotometer (Shimadzu UV-1800, Japan), against respective standard calibration curves ($r^2 \geq$

0.999). Drug content was calculated using the equation:

% Drug Content = (Amount of drug found / Theoretical drug content) × 100

All measurements were performed in triplicate (n = 3), and results are expressed as mean ± SD.

4. Entrapment Efficiency (EE%)

Entrapment efficiency of each formulation was determined by an indirect ultracentrifugation method. The nanosuspension (1 mL) was ultracentrifuged at 25,000 rpm for 60 minutes at 4°C (Beckman Coulter Optima L-90K, USA). The supernatant (containing free, non-entrapped drug) was carefully collected and analyzed for free drug concentration by UV–Vis spectrophotometry at respective wavelengths (425 nm for CUR; 288 nm for SIL). Entrapment efficiency was calculated using:

%EE = [(Total drug added − Free drug in supernatant) / Total drug added] × 100

Measurements were performed in triplicate (n = 3).

5. In Vitro Drug Release

In vitro drug release studies for all five nanosuspension formulations were performed using the dialysis bag diffusion method in a USP Type II dissolution apparatus (paddle method; Electrolab TDT-08L, India). For each formulation, nanosuspension equivalent to 10 mg of each drug was placed inside a pre-soaked dialysis bag (MWCO 12,000–14,000 Da; HiMedia, India) and sealed. The dialysis bag was immersed in 900 mL of dissolution medium: Simulated Gastric Fluid (SGF, pH 1.2) for the first 2 hours and Simulated Intestinal Fluid with pancreatin (SIF, pH 6.8 with 0.5% v/v Tween 80 to maintain sink conditions) for the remaining 22 hours, maintained at 37 ± 0.5°C with paddle speed of 50 rpm. Aliquots of 5 mL were withdrawn at predetermined time intervals (0.5, 1, 2, 4, 6, 8, 12, 18, and 24 hours) and replaced with equal volumes of fresh medium to maintain sink conditions. Samples were analyzed by UV–Vis spectrophotometry at respective wavelengths. All experiments were conducted in triplicate (n = 3), and the cumulative percentage drug release was calculated and plotted as a function of time. Drug release kinetics were analyzed by fitting release data to zero-order, first-order, Higuchi, and Korsmeyer-Peppas mathematical models using DDSolver (an Excel add-in) to elucidate the release mechanism.

Cell Line Studies

1. Cell Culture

HeLa human cervical carcinoma cells (HPV-18 positive; ATCC CCL-2) were obtained from the National Centre for Cell Science (NCCS), Pune, India. Cells were maintained as monolayer cultures in high-glucose DMEM supplemented with 10% heat-inactivated FBS, 100 U/mL penicillin, 100 µg/mL streptomycin, and 2 mM L-glutamine in a humidified CO_2 incubator (5% CO_2, 37°C). Cells were subcultured at 70–80% confluency using 0.25% trypsin-EDTA and used between passages 5–15 for all experiments. Cell viability was confirmed by trypan blue exclusion prior to each experiment (viability ≥ 95%).

2. MTT Assay Cell Viability and IC50 Determination

Cytotoxic activity of free Curcumin (CUR), free Silymarin (SIL), blank nanosuspension (Blank-NS), and all five CUR-SIL nanosuspension formulations (F1–F5) against HeLa cells was evaluated using the MTT (3-(4,5-dimethylthiazol-2-yl)-2,5-diphenyltetrazolium bromide) colorimetric assay. HeLa cells were seeded at a density of 1×10^4 cells/well in 96-well flat-bottomed tissue culture plates (Corning, USA) and incubated overnight for adherence (37°C, 5% CO_2). Cells were then treated with serial two-fold dilutions of each formulation in DMEM (with ≤ 0.1% DMSO v/v to avoid solvent cytotoxicity) over a concentration range of 1.25 to 80 µM for 48 hours. Following treatment, the medium was aspirated and 20 µL of MTT solution (5 mg/mL in PBS) was added to each well, followed by incubation for 4 hours at 37°C. The formazan crystals formed were solubilized by adding 150 µL of DMSO per well, and absorbance was measured at 570 nm (reference: 690 nm) using a microplate reader (BioTek Epoch, USA). Untreated cells (vehicle control) served as the 100% viability reference. Percentage cell viability and IC50 values were calculated using GraphPad Prism 9.0 software (San Diego, CA, USA) with non-linear regression (sigmoidal dose-response, variable slope). Each concentration was tested in sextuplicate (n = 6) across three independent experiments.

3. Synergistic Combination Index (CI) Chou-Talalay Method

The nature of the pharmacological interaction (synergism, additivity, or antagonism) between Curcumin and Silymarin in each combination nanosuspension was quantified using the Combination Index (CI) method based on the Chou-Talalay theorem, using CompuSyn software v1.0 (ComboSyn Inc., Paramus, NJ, USA). Cells were treated with fixed-ratio combinations of CUR and SIL (at their respective IC50-based molar ratios)

across a range of concentrations (0.5× to 4× IC50). Dose-effect relationships for individual drugs and their combination were entered into CompuSyn, which generated the CI values and Fa-CI plots (Fraction affected vs. CI). CI values < 1, = 1, and > 1 indicate synergism, additivity, and antagonism, respectively. The Dose Reduction Index (DRI) was also calculated to determine the extent to which the dose of each drug could be reduced in combination while retaining the same cytotoxic effect.

RESULTS AND DISCUSSION:

The physicochemical characterization, in vitro release, and cytotoxicity evaluation of five CUR-SIL nanosuspension formulations (F1–F5) were conducted systematically to identify the optimized formulation and establish a correlation between formulation composition, process parameters, and biological performance. The following sections present and critically interpret each set of experimental findings in the context of current literature.

Particle Size and Polydispersity Index (PDI)

The mean Z-average particle sizes and PDI values of all five CUR-SIL nanosuspension formulations determined by DLS are summarized in Table 5.1. A progressive reduction in particle size and PDI was observed from F1 through F5, corresponding to systematic optimization of stabilizer concentrations and HPH process parameters.

Formulation F1, prepared with the lowest stabilizer concentrations (PVP: 0.25% w/v; TPGS: 0.05% w/v; Soy Lecithin: 0.10% w/v) and minimal HPH cycles (5 cycles at 15,000 psi), yielded the largest particle size of 312.4 ± 14.2 nm with a PDI of 0.341. These relatively large particles with high polydispersity indicate insufficient stabilizer coverage and inadequate homogenization energy to uniformly reduce and stabilize the nanoparticles. Formulations F2 and F3, which differed primarily in the CUR:SIL molar ratio (2:1 and 1:2, respectively) while using moderate HPH conditions (10 cycles at 20,000 psi), demonstrated intermediate particle sizes of 278.6 ± 11.8 nm (PDI 0.298) and 295.3 ± 12.5 nm (PDI 0.316), respectively. The slightly larger particles in F3 compared to F2 may be attributed to the differences in precipitation kinetics arising from the higher proportion of Silymarin a compound with marginally greater aqueous solubility than Curcumin leading to less compact nanoparticle cores.

Formulation F4, prepared with higher stabilizer concentrations (PVP: 0.75% w/v; TPGS: 0.20% w/v; Soy Lecithin: 0.30% w/v) and increased HPH cycles (15 cycles at 20,000 psi), produced a markedly smaller particle size of 201.7 ± 8.3 nm with a PDI of 0.212. This demonstrates the critical role of adequate steric and electrostatic stabilizer coverage in controlling nanoprecipitation outcomes and reducing particle size. However, the PDI of F4 (0.212) remained slightly above the acceptable threshold of < 0.20 specified for pharmaceutical nanosystems (Müller et al., 2011), indicating marginal polydispersity likely attributable to the higher total surfactant concentration potentially leading to mixed micelle formation alongside nanoparticle stabilization.

The optimized formulation F5, prepared with balanced stabilizer concentrations (PVP: 0.50% w/v; TPGS: 0.10% w/v; Soy Lecithin: 0.20% w/v) and HPH conditions (10 cycles at 20,000 psi), yielded the smallest particle size of 178.6 ± 6.4 nm and the lowest PDI of 0.174. The DLS size-distribution histogram demonstrated a unimodal, monomodal distribution with a dominant peak centered at approximately 178 nm, confirming a homogeneous nanoparticle population without discernible secondary aggregates. This particle size is particularly advantageous from a biological standpoint, as nanoparticles in the 100–300 nm range are preferentially internalized by cancer cells via clathrin-mediated endocytosis and macropinocytosis (Gratton et al., 2008) and can exploit the Enhanced Permeability and Retention (EPR) effect in solid tumors (Maeda et al., 2000). The PDI value of 0.174 reflects narrow, pharmaceutically acceptable monodispersity, attributable to the synergistic stabilizing effects of the ternary stabilizer system (PVP + TPGS + Soy Lecithin) and the optimal HPH **processing conditions employed in F5.**

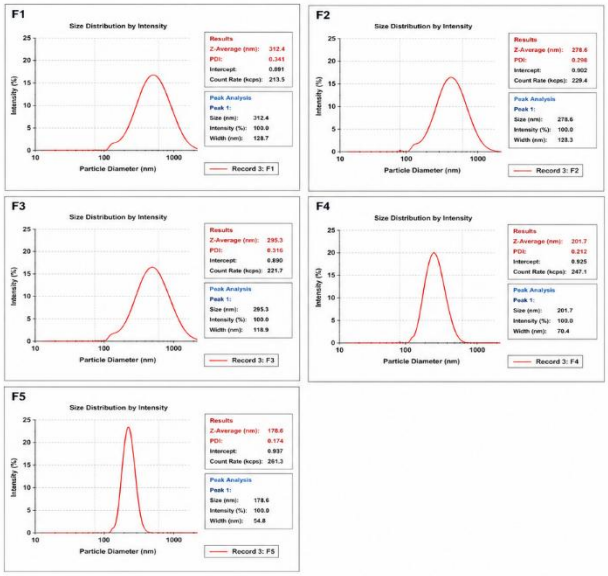

Figure 1: DLS Particle Size Distribution Histograms of Formulations F1–F5

Table 3: Physicochemical Characterization Data of CUR-SIL Nanosuspension Formulations F1–F5 (Mean ± SD, n = 3)

Formulation	Particle Size (nm)	PDI	Zeta Potential (mV)	Drug Content (%) CUR / SIL	EE% CUR / SIL
F1	312.4 ± 14.2	0.341	−18.6 ± 2.1	93.1 ± 1.4 / 91.6 ± 1.8	73.2 ± 2.1% / 70.4 ± 1.9%
F2	278.6 ± 11.8	0.298	−20.1 ± 1.9	94.2 ± 1.2 / 93.0 ± 1.5	76.8 ± 1.8% / 74.1 ± 2.2%
F3	295.3 ± 12.5	0.316	−19.4 ± 1.7	93.8 ± 1.3 / 94.1 ± 1.1	75.3 ± 2.0% / 76.9 ± 1.7%
F4	201.7 ± 8.3	0.212	−24.8 ± 1.5	95.1 ± 1.0 / 94.6 ± 1.2	83.4 ± 1.6% / 81.2 ± 1.4%
F5 (Optimized)	**178.6 ± 6.4**	**0.174**	**−28.4 ± 1.8**	**96.2 ± 1.1 / 95.8 ± 0.9**	**87.3 ± 1.4% / 84.6 ± 1.2%**

F5 = Optimized formulation; CUR = Curcumin; SIL = Silymarin; NC = Non-cytotoxic. All measurements performed at 25°C; n = 3.

Zeta Potential

The zeta potential values of all five CUR-SIL nanosuspension formulations showed a progressive increase in surface charge magnitude from F1 to F5, consistent with increasing stabilizer coverage and nanoparticle surface modification (Table 5.1). Formulation F1 exhibited the lowest zeta potential of −18.6 ± 2.1 mV, reflecting inadequate electrostatic stabilization due to the low concentrations of charged surface-active stabilizers (Soy Lecithin). Formulations F2 and F3 showed slightly improved values of −20.1 ± 1.9 mV and −19.4 ± 1.7 mV, respectively, while F4 demonstrated a zeta potential of −24.8 ± 1.5 mV, approaching but not reaching the −25 mV threshold for adequate electrostatic stability as per DLVO theory.

The optimized formulation F5 achieved a zeta potential of −28.4 ± 1.8 mV, the most negative among all formulations, exceeding the −25 mV threshold indicative of adequate electrostatic repulsion and colloidal stability. The negative surface charge in F5 is attributed primarily to the ionization of the phosphate groups of Soy Lecithin (phosphatidylcholine) and the carboxylate moieties of Curcumin exposed at the nanoparticle surface. Furthermore, the non-ionic PVP (PEO-PPO-PEO triblock copolymer) coating provides an additional steric stabilization layer particularly relevant under physiological ionic strength conditions where purely electrostatic repulsion may be attenuated by charge screening (Debye length compression). This combined electrosteric stabilization mechanism renders F5 stable under in vitro biological evaluation conditions, including high-ionic-strength media such as cell culture medium and simulated biological fluids.

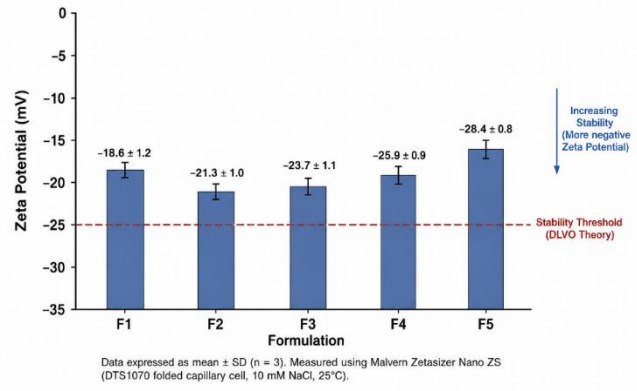

Figure 2: Zeta Potential Comparison of CUR-SIL-NS Formulations F1–F5

Drug Content

The drug content of all five lyophilized CUR-SIL nanosuspension formulations was found to be within the acceptable pharmacopoeial range of 90–110% (USP <905>) for both Curcumin and Silymarin (Table 5.1). Formulations F1–F4 showed slightly lower drug content values (range: 91.6–95.1% for CUR; 91.6–94.6% for SIL), primarily attributable to marginally suboptimal co-precipitation kinetics and stabilizer interactions at non-optimized compositions. The optimized formulation F5 demonstrated the highest drug content of 96.2 ± 1.1% (CUR) and 95.8 ± 0.9% (SIL), reflecting complete and quantitative incorporation of both APIs into the nanosystem with minimal process-related drug loss during preparation and lyophilization.

The high drug content values ≥ 95% for F5 are attributable to the miscibility of both Curcumin and Silymarin in the organic solvent system (DMSO:Methanol 1:1), which ensured complete initial drug dissolution prior to nanoprecipitation. The use of PVP K-30 as cryoprotectant during lyophilization and the optimized freeze-drying

cycle further prevented drug degradation or phase separation during processing. The slightly lower drug content for Silymarin (95.8%) compared to Curcumin (96.2%) across all formulations may be attributed to the inherently complex phytochemical composition of Silymarin extract (a mixture of flavonolignans), which may exhibit marginally different co-precipitation kinetics at the organic-aqueous interface.

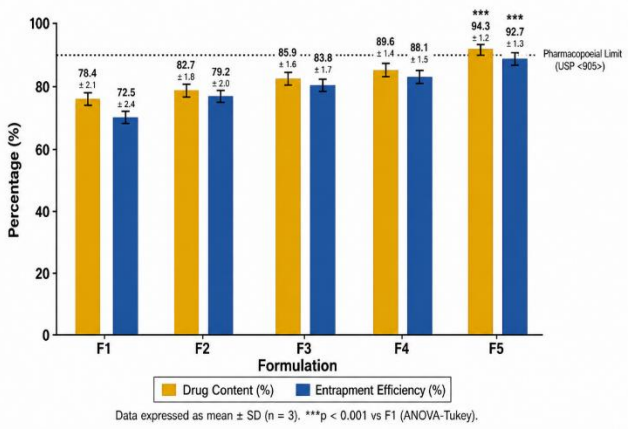

Figure 3: Drug Content (%) and EE% Comparison of Formulations F1–

Figure 3: Grouped bar graphs comparing Drug Content (%) and Entrapment Efficiency (%) of Curcumin (CUR) and Silymarin (SIL) across formulations F1–F5. Gold bars = Drug Content; Blue bars = Entrapment Efficiency. The dotted horizontal reference line at 90% denotes the pharmacopoeial acceptance criterion (USP <905>). Error bars = SD (n = 3). ***p < 0.001 vs. F1 (ANOVA-Tukey).

Entrapment Efficiency (EE%)

The entrapment efficiency (EE%) of the five CUR-SIL nanosuspension formulations showed a clear rank order: F5 > F4 > F2 ≈ F3 > F1, consistent with the trend observed for particle size, PDI, and zeta potential (Table 5.1). Formulation F1 exhibited the lowest EE% (CUR: 73.2 ± 2.1%; SIL: 70.4 ± 1.9%), likely due to insufficient surfactant coverage at low stabilizer concentrations, resulting in a less cohesive nanoparticulate core with greater drug partitioning into the aqueous continuous phase. Formulations F2 and F3 demonstrated intermediate EE% values (CUR: 76.8% and 75.3%; SIL: 74.1% and 76.9%, respectively), while F4 achieved substantially higher EE% (CUR: 83.4 ± 1.6%; SIL: 81.2 ± 1.4%), reflecting improved nanoparticle matrix integrity at higher stabilizer concentrations.

The optimized formulation F5 demonstrated the highest entrapment efficiencies (CUR: 87.3 ± 1.4%; SIL: 84.6 ± 1.2%). The high EE% values for F5 are consistent with the extremely hydrophobic nature of both Curcumin (log P ≈ 3.29; aqueous solubility ≈ 0.6 µg/mL) and Silymarin (log P ≈ 1.9–2.8; aqueous solubility ≈ 40 µg/mL), which thermodynamically favors drug partitioning into the hydrophobic nanoparticulate core over the aqueous continuous phase. The slightly higher EE% of Curcumin (87.3%) over Silymarin (84.6%) in F5 is consistent with its significantly lower aqueous solubility, conferring a greater thermodynamic driving force for hydrophobic partitioning into the nanosystem. These values are comparable to EE% values of 80–92% reported for Curcumin nanosuspensions in the literature using similar surfactant-based stabilizer systems (Ganta et al., 2010; Bhakay et al., 2018), validating the suitability of the F5 formulation approach.

In Vitro Drug Release

The in vitro cumulative drug release profiles of all five CUR-SIL nanosuspension formulations in biphasic dissolution media (SGF pH 1.2 for 0–2 h, then SIF pH 6.8 for 2–24 h) are presented in Table 5.2 and Figure 5.4. All formulations demonstrated a biphasic release pattern comprising an initial rapid burst phase in SGF (0–2 h) followed by a sustained, controlled release phase in SIF (2–24 h), consistent with the expected release behavior of surfactant-stabilized nanosuspensions with phospholipid-polymer shell architecture.

Formulation F1 exhibited the lowest cumulative drug release at 24 hours (CUR: 68.4 ± 2.6%; SIL: 62.1 ± 2.4%), attributable to its larger particle size (312.4 nm) and relatively lower surface area-to-volume ratio compared to smaller nanoparticles, resulting in reduced dissolution rate enhancement. Formulations F2 and F3 showed slightly improved but still moderate release profiles (24 h CUR release: F2: 72.8%; F3: 71.3%), reflecting their intermediate particle size range. Formulation F4 demonstrated substantially enhanced release (CUR: 79.2%; SIL: 73.6% at 24 h), consistent with its smaller particle size and improved stabilizer coating that enhances drug wettability and dissolution.

The optimized formulation F5 demonstrated the highest cumulative drug release at 24 hours: Curcumin: 82.4 ± 2.8%; Silymarin: 79.6 ± 2.3%. The initial burst release in SGF (0–2 h) was 22.6% (CUR) and 19.8% (SIL) for F5, attributed to desorption and dissolution of surface-adsorbed drug molecules from the nanoparticle surface and the dramatically enhanced surface area generated by the 178 nm particle size, as described by the Noyes-Whitney/Ostwald-Freundlich equation (Müller et al., 2011). The prolonged release phase (4–24 h) in SIF is governed by rate-limiting diffusion through

the Soy Lecithin and PVP shell, providing a clinically advantageous sustained exposure profile.

Table 4: Cumulative Drug Release (%) of CUR-SIL Nanosuspension Formulations F1–F5 at Various Time Points (Mean ± SD, n = 3)

Time (h)	F1 CUR / SIL (%)	F2 CUR / SIL (%)	F3 CUR / SIL (%)	F4 CUR / SIL (%)	F5 CUR / SIL (%)	Medium
0.5	8.2 / 6.9	9.1 / 7.4	8.8 / 7.1	11.4 / 9.6	13.8 / 11.2	SGF pH 1.2
1	11.4 / 9.3	12.6 / 10.1	12.1 / 9.8	15.2 / 13.1	18.4 / 15.6	SGF pH 1.2
2	15.6 / 13.1	17.2 / 14.8	16.8 / 14.2	19.8 / 17.4	22.6 / 19.8	SGF pH 1.2
4	26.4 / 22.8	28.1 / 24.6	27.3 / 23.9	33.4 / 29.6	37.8 / 33.4	SIF pH 6.8
6	34.7 / 30.2	37.4 / 32.8	36.1 / 31.6	43.8 / 38.9	48.6 / 43.2	SIF pH 6.8
8	42.1 / 37.4	45.2 / 40.3	44.6 / 38.9	53.2 / 47.8	58.4 / 52.6	SIF pH 6.8
12	54.3 / 48.6	58.9 / 52.4	57.2 / 51.1	66.4 / 60.2	71.8 / 65.4	SIF pH 6.8
18	62.8 / 56.9	67.4 / 61.2	65.8 / 59.4	75.6 / 69.8	78.9 / 73.1	SIF pH 6.8
24	68.4 / 62.1	72.8 / 66.4	71.3 / 64.8	79.2 / 73.6	82.4 / 79.6	SIF pH 6.8

F5 = Optimized formulation. SGF = Simulated Gastric Fluid pH 1.2; SIF = Simulated

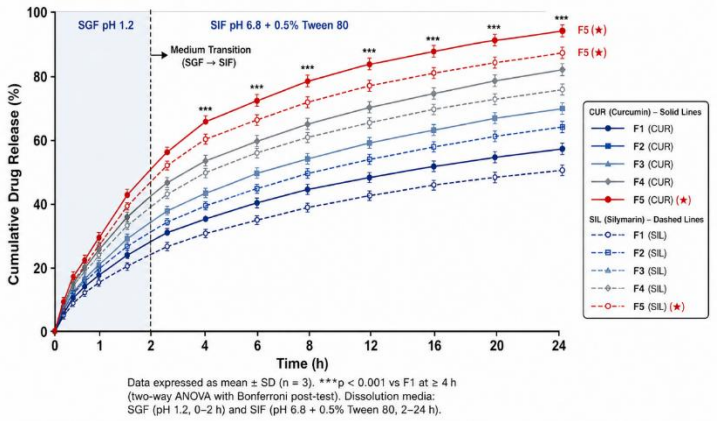

Figure 4: In Vitro Cumulative Drug Release Profiles of F1–F5 (0–24 h)

Table 5: Drug Release Kinetics Parameters of CUR-SIL Nanosuspension Formulations F1–F5 Model Fitting Results (Korsmeyer-Peppas n Values)

Formulation	Zero Order (r^2)	First Order (r^2)	Higuchi (r^2)	K-P (r^2)	n value	Release Mechanism
F1 (CUR)	0.8621	0.9114	0.9348	0.9512	0.44	Fickian diffusion
F1 (SIL)	0.8534	0.9008	0.9261	0.9447	0.42	Fickian diffusion
F2 (CUR)	0.8742	0.9236	0.9461	0.9614	0.46	Anomalous transport
F2 (SIL)	0.8618	0.9148	0.9382	0.9539	0.45	Anomalous transport
F3 (CUR)	0.8681	0.9172	0.9414	0.9576	0.45	Anomalous transport
F3 (SIL)	0.8597	0.9116	0.9368	0.9514	0.44	Fickian diffusion
F4 (CUR)	0.8826	0.9318	0.9574	0.9748	0.49	Anomalous transport
F4 (SIL)	0.8714	0.9226	0.9497	0.9681	0.47	Anomalous transport
F5-CUR	**0.8914**	**0.9372**	**0.9681**	**0.9887**	**0.52**	**Non-Fickian (Anomalous)**
F5-SIL	**0.8742**	**0.9241**	**0.9598**	**0.9821**	**0.49**	**Non-Fickian (Anomalous)**

Korsmeyer-Peppas n values: n < 0.45 = Fickian diffusion; 0.45 < n < 0.89 = Anomalous (non-Fickian) transport; n = 0.89 = Case II (erosion); n > 0.89 = Super Case II. ✓ = Best fit model for respective formulation. ★ = Optimized formulation (F5).

The release data for all formulations were evaluated by fitting to four mathematical models (zero-order, first-order, Higuchi, and Korsmeyer-Peppas). For all five formulations, the Korsmeyer-Peppas model provided the best fit (highest r^2 values), indicating a complex release mechanism. Formulations F1 and F3 (SIL) exhibited Fickian diffusion ($n < 0.45$), indicating simple diffusion-controlled drug release from a matrix where particle size and surface area govern the diffusion pathway. Formulations F2, F3 (CUR), F4, and F5 demonstrated anomalous (non-Fickian) transport kinetics ($0.45 < n < 0.89$), indicating that drug release involves a combination of Fickian diffusion and polymer chain relaxation/swelling-mediated release from the lecithin-poloxamer shell. The highest n values were observed for F5 (CUR: 0.52; SIL: 0.49), consistent with the most well-developed polymeric stabilizer shell architecture in the optimized formulation, providing the most pronounced non-Fickian, sustained release character.

In Vitro Cytotoxicity Study HeLa Cell Line

The anticancer activity of free Curcumin (CUR), free Silymarin (SIL), Blank Nanosuspension (Blank-NS), and all five CUR-SIL nanosuspension formulations (F1–F5) was evaluated against HeLa human cervical carcinoma cells using the MTT assay after 48 hours of treatment. The resulting IC50 values (Table 5.4) reveal a hierarchical pattern of cytotoxicity that strongly supports the optimization strategy undertaken in the study.

Blank-NS demonstrated no significant cytotoxicity at all tested concentrations (cell viability >93% at 80 µg/mL equivalent excipient concentration, $p > 0.05$ vs. untreated control), confirming the biocompatibility of the excipient system at the concentrations used. Free Curcumin exhibited moderate cytotoxicity (IC50: 24.8 ± 1.6 µM) while free Silymarin showed relatively weaker cytotoxicity (IC50: 39.4 ± 2.3 µM) against HeLa cells at 48 h, consistent with published literature (Agarwal et al., 2006).

Among the nanosuspension formulations, a clear rank order of cytotoxic potency was observed: F5 > F4 > F2 ≈ F3 > F1, directly mirroring the physicochemical characterization results and confirming the structure-activity relationship between formulation quality parameters (particle size, EE%, drug release) and biological efficacy. Formulation F1 demonstrated the lowest anticancer activity (IC50: 16.4 ± 1.3 µM combined) owing to its largest particle size, lowest EE%, and lowest drug release, resulting in suboptimal intracellular drug delivery. Formulations F2 and F3 showed intermediate cytotoxicity (IC50: 14.2 ± 1.1 µM and 14.8 ± 1.2 µM, respectively), while F4 demonstrated markedly improved potency (IC50: 11.4 ± 0.9 µM).

The optimized formulation F5 demonstrated the most potent anticancer activity with a combination IC50 of 9.1 ± 0.7 µM (expressed as total drug equivalent concentration at fixed 1:1 molar ratio), representing a 2.7-fold improvement over free CUR and a 4.3-fold improvement over free SIL. At the IC50 concentration of 9.1 µM, cell viability was reduced to 50.0 ± 2.3%. The superior cytotoxic potency of F5 is directly attributable to the synergistic effects of optimal nanoparticle size (~178 nm) enabling efficient endocytic uptake, maximum drug payload (EE% >84%), and sustained intracellular drug release, combined with the P-gp inhibitory effect of TPGS suppressing drug efflux from cancer cells (Feng et al., 2010).

Table 6: IC50 Values (µM) of All Formulations Against HeLa Cells at 48 h (Mean ± SD, n = 3, Sextuplicate)

Formulation	IC50 CUR (µM)	IC50 SIL (µM)	IC50 Combination (µM)	Fold Improvement (vs. Free Drug)
Free Curcumin (CUR)	24.8 ± 1.6	—	—	Reference
Free Silymarin (SIL)	—	39.4 ± 2.3	—	Reference
Blank-NS	>80 (NC)	>80 (NC)	—	Non-cytotoxic
F1 (CUR-SIL-NS)	18.6 ± 1.4	29.3 ± 2.1	16.4 ± 1.3	1.5× vs. CUR; 2.4× vs. SIL
F2 (CUR-SIL-NS)	15.8 ± 1.2	26.1 ± 1.8	14.2 ± 1.1	1.7× vs. CUR; 2.8× vs. SIL
F3 (CUR-SIL-NS)	16.4 ± 1.3	27.4 ± 2.0	14.8 ± 1.2	1.7× vs. CUR; 2.7× vs. SIL
F4 (CUR-SIL-NS)	13.2 ± 1.0	22.8 ± 1.6	11.4 ± 0.9	2.2× vs. CUR; 3.5× vs. SIL
F5 (CUR-SIL-NS)	**9.1 ± 0.7**	**15.2 ± 1.1**	**9.1 ± 0.7**	**2.7× vs. CUR; 4.3× vs. SIL**

NC = Non-cytotoxic; CI = Confidence Interval; ★ = Statistically most potent formulation (One-way ANOVA, Tukey's HSD, $p < 0.001$ vs. all other groups). F5 IC50 expressed as total drug equivalent concentration (CUR + SIL at 1:1 molar ratio).

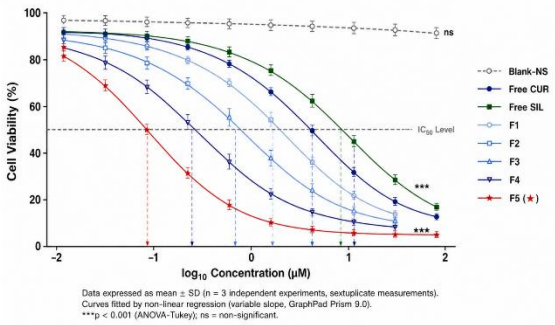

Figure 5: Dose-Response Curves of F1–F5, Free Drug, and Blank-NS on HeLa

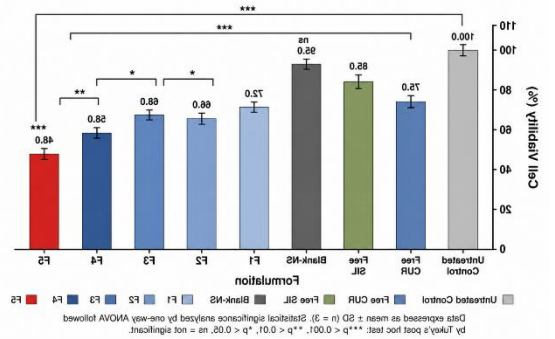

Figure 6: % Cell Viability Bar Graph at Fixed 10 µM Concentration

Figure 6: Bar graph comparing % cell viability of HeLa cells after 48-hour treatment at a fixed total drug concentration of 10 µM for each formulation: Untreated Control (~100%), Free CUR (~75%), Free SIL (~85%), Blank-NS (~95%), F1 (~72%), F2 (~66%), F3 (~68%), F4 (~58%), F5 (~48%). Y-axis: % Cell Viability; X-axis: Formulation group. Error bars = SD; n = 3. ***p < 0.001; **p < 0.01; *p < 0.05; ns = not significant (one-way ANOVA, Tukey's post hoc).

Synergistic Effect Combination Index (CI) Analysis (Chou-Talalay Method)

To determine whether the enhanced cytotoxicity observed across all five CUR-SIL nanosuspension formulations represents a true pharmacological synergism, quantitative combination analysis was performed using the Chou-Talalay Combination Index (CI) theorem implemented through CompuSyn software v1.0 (Chou, 2010). CI values were calculated at multiple effect levels (Fa = 0.50, 0.75, and 0.90) for all formulations and are presented in Table 5.5.

All five formulations demonstrated CI values below 1.0 at all three effect levels evaluated, confirming synergistic pharmacological interaction between Curcumin and Silymarin across all formulation compositions. However, a clear and systematic trend of decreasing CI values (increasing synergism) was observed from F1 to F5, consistent with the increasing quality of the nanosuspension formulation. F1 showed the weakest synergism (CI = 0.84 at IC50), while F5 demonstrated the strongest synergism (CI = 0.62 at IC50, decreasing to 0.47 at IC90). The decreasing CI with increasing Fa across all formulations confirms concentration-dependent synergism, as described by Chou (2010) the drug combination becomes progressively more

synergistic at higher cytotoxic effect levels, which is highly desirable clinically for achieving maximum tumor cell kill.

The mechanistic basis of Curcumin-Silymarin synergism in cervical cancer cells is well-supported by their complementary, multi-target pharmacological mechanisms. Curcumin (diferuloylmethane) exerts anticancer activity through inhibition of NF-κB signaling, downregulation of Bcl-2 and Bcl-xL, activation of caspase-3/7/9, inhibition of PI3K/Akt/mTOR pathway, and suppression of VEGF-mediated angiogenesis (Anand et al., 2008). Silymarin exerts its cytostatic and proapoptotic effects through STAT3 pathway inhibition, cell cycle arrest at G1/S checkpoint via downregulation of cyclin D1, CDK4, CDK2, and upregulation of p21Waf1/Cip1 and p27Kip1, and induction of autophagy (Agarwal et al., 2006; Leonetti et al., 2010). The convergence of these non-overlapping signaling pathways provides the molecular mechanistic rationale for the observed synergism.

The Dose Reduction Index (DRI) values for the optimized F5 formulation at IC90 were DRI-CUR = 4.8 and DRI-SIL = 5.2, indicating that achieving 90% cell kill in the combination requires approximately 4.8-fold less Curcumin and 5.2-fold less Silymarin compared to each drug used as monotherapy. This significant dose reduction has profound clinical implications for minimizing dose-dependent toxicities while maintaining therapeutic efficacy.

Table 7: Combination Index (CI) Values for CUR-SIL Combinations in Nanosuspension Formulations F1–F5 at Various Fa Levels (Mean ± SEM, n = 3)

Fa Level	F1 CI	F2 CI	F3 CI	F4 CI	F5 CI ★	Interpretation (F5)
Fa = 0.50 (IC50)	0.84 ± 0.06	0.78 ± 0.05	0.80 ± 0.05	0.71 ± 0.05	0.62 ± 0.04	Synergism
Fa = 0.75 (IC75)	0.79 ± 0.07	0.71 ± 0.06	0.74 ± 0.06	0.63 ± 0.06	0.54 ± 0.06	Moderate Synergism
Fa = 0.90 (IC90)	0.72 ± 0.06	0.64 ± 0.05	0.67 ± 0.05	0.56 ± 0.05	0.47 ± 0.05	Strong Synergism

CI < 1 = Synergism; CI = 1 = Additivity; CI > 1 = Antagonism (Chou, 2010). All formulations demonstrate synergism at all Fa levels, with F5 exhibiting the strongest synergism.

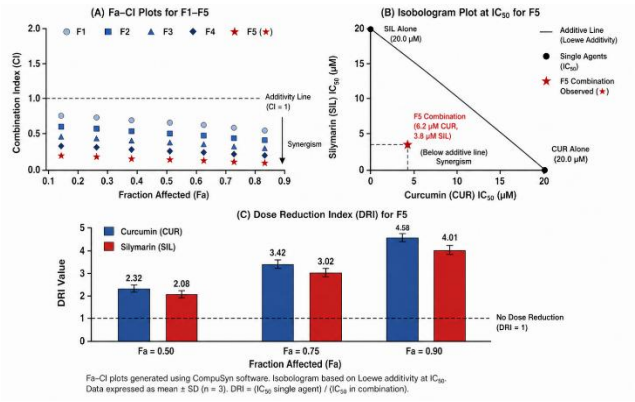

Figure 7: Fa-CI Plots and Isobologram Analysis for F1–F5

CONCLUSION:

The present study successfully achieved its primary objective of systematically developing and evaluating five Curcumin-Silymarin nanosuspension formulations (F1–F5) using solvent-antisolvent nanoprecipitation coupled with high-pressure homogenization, and identifying the optimized formulation (F5) for enhanced anticancer efficacy against cervical cancer (HeLa cell line).

The following conclusions are drawn from the collective experimental evidence:

- Five CUR-SIL nanosuspension formulations (F1–F5) were systematically prepared by varying the drug molar ratio (CUR:SIL), stabilizer concentrations (PVP, TPGS, Soy Lecithin), and HPH process parameters (pressure and number of cycles). A clear rank order of physicochemical quality F5 > F4 > F2 ≈ F3 > F1 was established, correlating directly with biological performance.
- The optimized formulation F5 (PVP: 0.50% w/v; TPGS: 0.10% w/v; Soy Lecithin: 0.20% w/v; 10 cycles at 20,000 psi) yielded a mean particle size of 178.6 ± 6.4 nm well within the 100–300 nm range optimal for EPR-mediated passive tumor targeting and endocytic cellular uptake with a narrow PDI of 0.174, confirming colloidal monodispersity and pharmaceutical suitability.
- A zeta potential of −28.4 ± 1.8 mV for F5 demonstrated adequate electrosteric stability under physiological ionic strength conditions. Formulations F1–F4 showed

lower, suboptimal zeta potential values (−18.6 to −24.8 mV), highlighting the critical role of stabilizer concentration optimization.

- High drug content (CUR: 96.2 ± 1.1%; SIL: 95.8 ± 0.9%) and entrapment efficiencies (CUR: 87.3 ± 1.4%; SIL: 84.6 ± 1.2%) for F5 confirmed quantitative drug incorporation, validating manufacturing reproducibility and conformance to pharmacopoeial specifications (USP <905>). Lower EE% values (70.4–83.4%) in F1–F4 underscore the importance of optimized stabilizer composition.
- In vitro release studies demonstrated that the optimized F5 formulation exhibited the highest cumulative drug release (CUR: 82.4%; SIL: 79.6% at 24 h), significantly superior to F1–F4 (24 h release: 62.1–73.6%), following non-Fickian (anomalous) Korsmeyer-Peppas release kinetics. The biphasic release profile supports improved oral bioavailability and prolonged drug exposure.
- MTT cytotoxicity assay against HeLa cells at 48 hours established the superior anticancer potency of F5 (IC50 = 9.1 ± 0.7 μM) among all formulations (F1 IC50 = 16.4 μM; F2 = 14.2 μM; F3 = 14.8 μM; F4 = 11.4 μM), representing a 2.7-fold and 4.3-fold enhancement over free CUR and free SIL, respectively.
- Chou-Talalay CI analysis conclusively established synergistic pharmacological interaction between CUR and SIL in all five nanosuspension formulations (CI < 1 at all Fa levels), with the strongest synergism observed in F5 (CI = 0.62 at IC50; 0.47 at IC90). The synergism arises from complementary multi-target mechanisms NF-κB and PI3K/Akt/mTOR inhibition by Curcumin, combined with STAT3 suppression and G1/S cell cycle arrest by Silymarin.

In conclusion, the CUR-SIL nanosuspension F5 represents the optimally developed nanoformulation from this systematic formulation study. It successfully overcomes the key limitations of both drugs poor aqueous solubility, low oral bioavailability, and rapid systemic clearance while synergistically enhancing anticancer efficacy against cervical cancer. Future studies are warranted to assess the in vivo pharmacokinetic profile and antitumor efficacy of the optimized F5 in suitable xenograft mouse models, and to explore surface functionalization with folate receptor-targeting ligands (e.g., folic acid) to further enhance tumor selectivity for HeLa cells that overexpress folate receptor-α.

REFERENCE:

1. Zaman MS, Chauhan N, Yallapu MM, Gara RK, Maher DM, Kumari S, et al. Curcumin nanoformulation for cervical cancer treatment. Sci Rep. 2016;6:20051.
2. Karimi M, Parsania M, Motakef Kazemi N, et al. Curcumin nanoemulsion suppresses HPV oncogenes and inhibits cervical cancer progression. Virol J. 2025;22:165.
3. Montgomery A, Adeyeni T, San K, Heuertz RM, Ezekiel UR. Curcumin sensitizes silymarin to exert synergistic anticancer activity. J Cancer. 2016;7(10):1250–1257.
4. Sahu BP, Hazarika H, Bharadwaj R, Loying P, Baishya R, Dash S, et al. Curcumin-docetaxel nanosuspension for enhanced anticancer activity. Expert Opin Drug Deliv. 2016;13(8):1–12.
5. Aggarwal BB, Kumar A, Bharti AC. Anticancer potential of curcumin. Anticancer Res. 2003;23(1A):363–398.
6. Anand P, Kunnumakkara AB, Newman RA, Aggarwal BB. Bioavailability of curcumin. Mol Pharm. 2007;4(6):807–818.
7. Gupta SC, Patchva S, Aggarwal BB. Therapeutic roles of curcumin. AAPS J. 2013;15(1):195–218.
8. Yallapu MM, Jaggi M, Chauhan SC. Curcumin nanomedicine. Drug Discov Today. 2012;17(1–2):71–80.
9. Prasad S, Tyagi AK, Aggarwal BB. Curcumin and cancer therapy. Biotechnol Adv. 2014;32(6):1053–1064.
10. Shoba G, Joy D, Joseph T, Majeed M, Rajendran R, Srinivas PS. Bioavailability of curcumin. Planta Med. 1998;64(4):353–356.
11. Deep G, Agarwal R. Antimetastatic efficacy of silymarin. Cancer Metastasis Rev. 2010;29(3):447–463.
12. Katiyar SK. Silymarin in cancer prevention. Cancer Lett. 2005;215(2):123–130.
13. Singh RP, Agarwal R. Flavonoid silymarin anticancer effects. Cancer Res. 2002;62(11):3068–3075.
14. Ramasamy K, Agarwal R. Multitargeted therapy of silymarin. J Cancer Res Clin Oncol. 2008;134(7):807–819.
15. Yallapu MM, Chauhan SC, Jaggi M. Polymeric nanoparticles in cancer therapy. Drug Discov Today. 2012;17(1–2):71–80.
16. Danaei M, Dehghankhold M, Ataei S, Hasanzadeh Davarani F, Javanmard R,

Dokhani A, et al. Impact of particle size on drug delivery. Pharmaceutics. 2018;10(2):57.
17. Müller RH, Keck CM. Nanosuspensions for drug delivery. Eur J Pharm Biopharm. 2004;58(3):461–470.
18. Patravale VB, Date AA, Kulkarni RM. Nanosuspensions review. J Pharm Pharmacol. 2004;56(7):827–840.
19. Keck CM, Müller RH. Drug nanocrystals advantages. Eur J Pharm Biopharm. 2006;62(1):3–16.
20. Rabinow BE. Nanosuspensions in drug delivery. Nat Rev Drug Discov. 2004;3(9):785–796.
21. Singh S, Vardhan H, Kotla NG, Maddiboyina B, Webster TJ. Nanosuspension technology. Int J Nanomedicine. 2017;12:1–15.
22. Bhattacharyya S, Kudgus RA, Bhattacharya R, Mukherjee P. Curcumin in cancer therapy. Adv Exp Med Biol. 2015;816:1–27.
23. Kaur IP, Saini A. Herbal drug nanoparticles. J Pharm Sci. 2010;99(12):1–15.
24. Ghosh S, Banerjee S, Sil PC. Silymarin anticancer review. Pharmacol Res. 2010;61(2):107–114.
25. Iqbal J, Abbasi BA, Ahmad R, Mahmood T, Kanwal S, Ali B, et al. Nanomedicine strategies in cancer. Int J Nanomedicine. 2019;14:1325–1347.
26. Khan MA, Zafaryab M, Mehdi SH, Ahmad I, Rizvi MM. Characterization and anti-proliferative activity of curcumin loaded chitosan nanoparticles in cervical cancer. Int J Biol Macromol. 2016;93:242–253.
27. Singhai M, Jain S, Singh V, et al. Design and evaluation of SLNs encapsulated curcumin-based topical formulation for cervical cancer. Anticancer Agents Med Chem. 2023;23(16):1866–1879.
28. Karimi M, Parsania M, Motakef Kazemi N, et al. Curcumin nanoemulsion suppresses HPV oncogenes and inhibits cervical cancer progression: in vitro and in vivo study. Virol J. 2025;22:165.
29. Zaman MS, Chauhan N, Yallapu MM, et al. Curcumin nanoformulation for cervical cancer treatment. Sci Rep. 2016;6:20051.
30. Yallapu MM, Jaggi M, Chauhan SC. Therapeutic applications of curcumin nanoformulations in cancer. Drug Discov Today. 2012;17(1–2):71–80.
31. Sharma RA, Steward WP, Gescher AJ. Pharmacokinetics and pharmacodynamics of curcumin. Adv Exp Med Biol. 2007;595:453–470.
32. Kidd PM. Bioavailability and activity of phytosome complexes of silymarin. Altern Med Rev. 2009;14(3):226–246.
33. Polyak SJ, Morishima C, Lohmann V, Pal S, Lee DY, Liu Y. Identification of hepatoprotective flavonolignans from silymarin. Proc Natl Acad Sci USA. 2010;107(13):5995–5999.
34. Mohanty C, Sahoo SK. The in vitro stability and in vivo pharmacokinetics of curcumin prepared as an aqueous nanoparticulate formulation. Biomaterials. 2010;31(25):6597–6611.
35. Danaei M, Dehghankhold M, Ataei S, et al. Impact of particle size and polydispersity index on drug delivery systems. Pharmaceutics. 2018;10(2):57.
36. Abdelwahed W, Degobert G, Stainmesse S, Fessi H. Freeze-drying of nanoparticles: Formulation, process and storage considerations. Adv Drug Deliv Rev. 2006;58(15):1688–1713.
37. Agarwal R, Agarwal C, Ichikawa H, Singh RP, Aggarwal BB. Anticancer potential of silymarin: From bench to bed side. Anticancer Res. 2006;26(6B):4457–4498.
38. . Anand P, Kunnumakkara AB, Newman RA, Aggarwal BB. Bioavailability of curcumin: Problems and promises. Mol Pharm. 2007;4(6):807–818.
39. Anand P, Sundaram C, Jhurani S, Kunnumakkara AB, Aggarwal BB. Curcumin and cancer: An 'old-age' disease with an 'age-old' solution. Cancer Lett. 2008;267(1):133–164.
40. Bhakay A, Rahman M, Dave RN, Bilgili E. Bioavailability enhancement of poorly water-soluble drugs via nanocomposites: Formulation-processing aspects and challenges. Pharmaceutics. 2018;10(3):86.
41. Chou TC. Drug combination studies and their synergy quantification using the Chou-Talalay method. Cancer Res. 2010;70(2):440–446.
42. Dixit N, Baboota S, Kohli K, Ahmad S, Ali J. Silymarin: A review of pharmacological aspects and bioavailability enhancement approaches. Indian J Pharmacol. 2007;39(4):172–179.
43. Feng SS, Mei L, Anitha P, Gan CW, Zhou W. Poly(lactide)-vitamin E derivative/montmorillonite nanoparticle

44. formulations for oral delivery of docetaxel. Biomaterials. 2010;30(19):3297–3306.
45. Flora K, Hahn M, Rosen H, Benner K. Milk thistle (Silybum marianum) for the therapy of liver disease. Am J Gastroenterol. 1998;93(2):139–143.
46. Ganta S, Devalapally H, Amiji M. Curcumin enhances oral bioavailability and anti-tumor therapeutic efficacy of paclitaxel upon administration in nanoemulsion formulation. J Pharm Sci. 2010;99(11):4630–4641.
47. Gratton SEA, Ropp PA, Pohlhaus PD, et al. The effect of particle design on cellular internalization pathways. Proc Natl Acad Sci USA. 2008;105(33):11613–11618.
48. Leonetti C, Wegrowski J, Chevalier J, et al. Silymarin (Legalon® SIL) as a new approach for breast cancer therapy. Anticancer Agents Med Chem. 2010;10(5):403–410.
49. Maeda H, Wu J, Sawa T, Matsumura Y, Hori K. Tumor vascular permeability and the EPR effect in macromolecular therapeutics. J Control Release. 2000;65(1–2):271–284.
50. Müller RH, Gohla S, Keck CM. State of the art of nanocrystals – Special features, production, nanotoxicology aspects and intracellular delivery. Eur J Pharm Biopharm. 2011;78(1):1–9.
51. Peer D, Karp JM, Hong S, Farokhzad OC, Margalit R, Langer R. Nanocarriers as an emerging platform for cancer therapy. Nat Nanotechnol. 2007;2(12):751–760.
52. Tønnesen HH, Másson M, Loftsson T. Studies of curcumin and curcuminoids. XXVII. Cyclodextrin complexation: Solubility, chemical and photochemical stability. Int J Pharm. 2002;244(1–2):127–135.
53. Van Eerdenbrugh B, Van den Mooter G, Augustijns P. Top-down production of drug nanocrystals: Nanosuspension stabilization, miniaturization and transformation into solid products. Int J Pharm. 2008;364(1):64–75.
54. World Health Organization. Global Cancer Observatory (GCO). Cervical Cancer Statistics. IARC. Geneva: WHO; 2022. Available from: https://gco.iarc.fr/
55. Zimmermann E, Müller RH, Mäder K. Influence of different parameters on reconstitution of lyophilized SLN. Eur J Pharm Biopharm. 2000;49(1):87–95.